THE SLOAN DIGITAL SKY SURVEY-II SUPERNOVA SURVEY: TECHNICAL SUMMARY

JOSHUA A. FRIEMAN[1,2,3], BRUCE BASSETT[4,5], ANDREW BECKER[6], CHANGSU CHOI[7], DAVID CINABRO[8], FRITZ DEJONGH[1],
DARREN L. DEPOY[9], BEN DILDAY[2,10], MAMORU DOI[11], PETER M. GARNAVICH[12], CRAIG J. HOGAN[6], JON HOLTZMAN[13],
MYUNGSHIN IM[7], SAURABH JHA[14], RICHARD KESSLER[2,15], KOHKI KONISHI[16], HUBERT LAMPEITL[17], JOHN MARRINER[1],
JENNIFER L. MARSHALL[9], DAVID MCGINNIS[1], GAJUS MIKNAITIS[1], ROBERT C. NICHOL[18], JOSE LUIS PRIETO[9], ADAM G. RIESS[17,19],
MICHAEL W. RICHMOND[20], ROGER ROMANI[14], MASAO SAKO[21], DONALD P. SCHNEIDER[22], MATHEW SMITH[18],
NAOHIRO TAKANASHI[11], KOUICHI TOKITA[11], KURT VAN DER HEYDEN[5], NAOKI YASUDA[16], CHEN ZHENG[14],
JENNIFER ADELMAN-MCCARTHY[1], JAMES ANNIS[1], ROBERTO J. ASSEF[9], JOHN BARENTINE[23,24], RALF BENDER[25,26],
ROGER D. BLANDFORD[14], WILLIAM N. BOROSKI[1], MALCOLM BREMER[27], HOWARD BREWINGTON[24], CHRIS A. COLLINS[28],
ARLIN CROTTS[29], JACK DEMBICKY[24], JASON EASTMAN[9], ALASTAIR EDGE[30], EDMOND EDMONDSON[18], EDWARD ELSON[5],
MICHAEL E. EYLER[31], ALEXEI V. FILIPPENKO[32], RYAN J. FOLEY[32], STEPHAN FRANK[9], ARIEL GOOBAR[33], TINA GUETH[13],
JAMES E. GUNN[34], MICHAEL HARVANEK[24,35], ULRICH HOPP[25,26], YUTAKA IHARA[11], ŽELKO IVEZIĆ[6], STEVEN KAHN[14],
JARED KAPLAN[36], STEPHEN KENT[1,3], WILLIAM KETZEBACK[24], SCOTT J. KLEINMAN[24,37], WOLFRAM KOLLATSCHNY[38],
RICHARD G KRON[3], JUREK KRZESIŃSKI[24,39], DENNIS LAMENTI[40], GIORGOS LELOUDAS[41], HUAN LIN[1], DANIEL C. LONG[24],
JOHN LUCEY[30], ROBERT H. LUPTON[34], ELENA MALANUSHENKO[24], VIKTOR MALANUSHENKO[24], RUSSET J. MCMILLAN[24],
JAVIER MENDEZ[42], CHRISTOPHER W. MORGAN[9,31], TOMOKI MOROKUMA[11,43], ATSUKO NITTA[24,44], LINDA OSTMAN[33], KAIKE PAN[24],
CONSTANCE M. ROCKOSI[45], A. KATHY ROMER[46], PILAR RUIZ-LAPUENTE[42], GABRELLE SAURAGE[24], KATIE SCHLESINGER[9],
STEPHANIE A. SNEDDEN[24], JESPER SOLLERMAN[41,47], CHRIS STOUGHTON[1], MAXIMILIAN STRITZINGER[41], MARK SUBBARAO[3],
DOUGLAS TUCKER[1], PETRI VAISANEN[5], LINDA C. WATSON[9], SHANNON WATTERS[24], J. CRAIG WHEELER[23], BRIAN YANNY[1], AND
DONALD YORK[3,15]

[1] Center for Particle Astrophysics, Fermi National Accelerator Laboratory, P.O. Box 500, Batavia, IL 60510, USA
[2] Kavli Institute for Cosmological Physics, The University of Chicago, 5640 South Ellis Avenue Chicago, IL 60637, USA
[3] Department of Astronomy and Astrophysics, The University of Chicago, 5640 South Ellis Avenue, Chicago, IL 60637, USA
[4] Department of Mathematics and Applied Mathematics, University of Cape Town, Rondebosch 7701, South Africa
[5] South African Astronomical Observatory, P.O. Box 9, Observatory 7935, South Africa
[6] Department of Astronomy, University of Washington, Box 351580, Seattle, WA 98195, USA
[7] Department of Astronomy, Seoul National University, Seoul, South Korea
[8] Department of Physics, Wayne State University, Detroit, MI 48202, USA
[9] Department of Astronomy, Ohio State University, 140 West 18th Avenue, Columbus, OH 43210-1173, USA
[10] Department of Physics, University of Chicago, Chicago, IL 60637, USA
[11] Institute of Astronomy, Graduate School of Science, University of Tokyo 2-21-1, Osawa, Mitaka, Tokyo 181-0015, Japan
[12] University of Notre Dame, 225 Nieuwland Science, Notre Dame, IN 46556-5670, USA
[13] Department of Astronomy, MSC 4500, New Mexico State University, P.O. Box 30001, Las Cruces, NM 88003, USA
[14] Kavli Institute for Particle Astrophysics & Cosmology, Stanford University, Stanford, CA 94305-4060, USA
[15] Enrico Fermi Institute, University of Chicago, 5640 South Ellis Avenue, Chicago, IL 60637, USA
[16] Institute for Cosmic Ray Research, University of Tokyo, 5-1-5, Kashiwanoha, Kashiwa, Chiba, 277-8582, Japan
[17] Space Telescope Science Institute, 3700 San Martin Drive, Baltimore, MD 21218, USA
[18] Institute of Cosmology and Gravitation, Mercantile House, Hampshire Terrace, University of Portsmouth, Portsmouth PO1 2EG, UK
[19] Department of Physics and Astronomy, Johns Hopkins University, 3400 North Charles Street, Baltimore, MD 21218, USA
[20] Physics Department, Rochester Institute of Technology, 85 Lomb Memorial Drive, Rochester, NY 14623-5603, USA
[21] Department of Physics and Astronomy, University of Pennsylvania, 203 South 33rd Street, Philadelphia, PA 19104, USA
[22] Department of Astronomy and Astrophysics, The Pennsylvania State University, 525 Davey Laboratory, University Park, PA 16802, USA
[23] Department of Astronomy, McDonald Observatory, University of Texas, Austin, TX 78712, USA
[24] Apache Point Observatory, P.O. Box 59, Sunspot, NM 88349, USA
[25] Universitaets-Sternwarte Munich, 1 Scheinerstr, Munich, D-81679, Germany
[26] Max Planck Institute for Extraterrestrial Physics, D-85748, Garching, Munich, Germany
[27] H. H. Wills Physics Laboratory, University of Bristol, Bristol, BS8 1TL, UK
[28] Astrophysics Research Institute, Liverpool John Moores University, Birkenhead CH41 1LD, UK
[29] Department of Astronomy, Columbia University, New York, NY 10027, USA
[30] Department of Physics, University of Durham, South Road, Durham, DH1 3LE, UK
[31] Department of Physics, United States Naval Academy, 572C Holloway Road, Annapolis, MD 21402, USA
[32] Department of Astronomy, University of California, Berkeley, CA 94720-3411, USA
[33] Physics Department, Stockholm University, AlbaNova University Center, 106 91 Stockholm, Sweden
[34] Princeton University Observatory, Peyton Hall, Princeton, NJ 08544, USA
[35] Lowell Observatory, 1400 Mars Hill Rd., Flagstaff, AZ 86001, USA
[36] Jefferson Laboratory of Physics, Harvard University, Cambridge, MA 02138, USA
[37] Subaru Telescope, 650 North A'ohoku Place, Hilo, HI 96720, USA
[38] Institut für Astrophysik, Universität Göttingen, Friedrich-Hund-Platz 1, D-37077 Göttingen, Germany
[39] Obserwatorium Astronomiczne na Suhorze, Akademia Pedagogiczna w Krakowie, ulica Podchorążych 2, PL-30-084 Kraków, Poland
[40] Department of Physics & Astronomy, San Francisco State University, San Francisco, CA 94132-4163, USA
[41] Dark Cosmology Centre, Niels Bohr Institute, University of Copenhagen, DK-2100, Denmark
[42] Department of Astronomy, University of Barcelona, Marti i Franques 1, E-08028 Barcelona, Spain
[43] National Astronomical Observatory of Japan, 2-21-1, Osawa, Mitaka, Tokyo 181-8588, Japan
[44] Gemini Observatory, 670 North A'ohoku Place, Hilo, HI 96720, USA
[45] Lick Observatory, University of California, Santa Cruz, CA 95064, USA
[46] Astronomy Center, University of Sussex, Falmer, Brighton BN1 9QJ, UK
[47] Astronomy Department, Stockholm University, AlbaNova University Center, 106 91 Stockholm, Sweden

ABSTRACT

The Sloan Digital Sky Survey-II (SDSS-II) has embarked on a multi-year project to identify and measure light curves for intermediate-redshift ($0.05 < z < 0.35$) Type Ia supernovae (SNe Ia) using repeated five-band (*ugriz*) imaging over an area of 300 sq. deg. The survey region is a stripe $2.5°$ wide centered on the celestial equator in the Southern Galactic Cap that has been imaged numerous times in earlier years, enabling construction of a deep reference image for the discovery of new objects. Supernova imaging observations are being acquired between September 1 and November 30 of 2005–7. During the first two seasons, each region was imaged on average every five nights. Spectroscopic follow-up observations to determine supernova type and redshift are carried out on a large number of telescopes. In its first two three-month seasons, the survey has discovered and measured light curves for 327 spectroscopically confirmed SNe Ia, 30 probable SNe Ia, 14 confirmed SNe Ib/c, 32 confirmed SNe II, plus a large number of photometrically identified SNe Ia, 94 of which have host-galaxy spectra taken so far. This paper provides an overview of the project and briefly describes the observations completed during the first two seasons of operation.

Key words: supernovae: general – surveys

Online-only material: color figures

1. INTRODUCTION

Type Ia supernovae (SNe Ia) are now well established as the method of choice for accurate relative distance determination over cosmological scales (see, e.g., Leibundgut 2001; Filippenko 2005). However, present cosmological constraints are based upon a Hubble diagram constructed from low- and high-redshift SN Ia samples that have been observed with a variety of telescopes, instruments, and photometric passbands. Photometric offsets between these samples are highly degenerate with changes in cosmological parameters and could be hidden in part because there is a gap or "redshift desert" between the nearby ($z \lesssim 0.1$) and distant ($z \gtrsim 0.3$) samples; e.g., only 6 of the 157 *high-quality* SN Ia light curves comprising the "Gold sample" used by Riess et al. (2004) fall in this gap. In addition, the low-redshift SN measurements used to anchor the Hubble diagram themselves were compiled from combinations of several nearby surveys using different telescopes, instruments, and selection criteria. While supernovae provided the first indications for the accelerating Universe (Riess et al. 1998; Perlmutter et al. 1999), obtaining precise constraints on the nature of the dark energy will require much improved control over such sources of systematic errors. Increasing precision calls for larger supernova samples with continuous redshift coverage of the Hubble diagram; it also necessitates *high-quality* data, with densely-sampled, multi-band SN light curves and well-understood photometric calibration.

The Sloan Digital Sky Survey-II Supernova (SDSS-II SN) Survey, one of the three components of the SDSS-II project, is designed to address both the paucity of SN Ia data at intermediate redshifts and the systematic limitations of previous SN Ia samples, thereby leading to more robust constraints upon the properties of the dark energy (for a description of the SDSS, see York et al. 2000). With its unique combination of large areal coverage, sensitivity, and photometric accuracy, the SDSS has the ability to bridge the redshift desert and aims to discover and measure high-quality light curves for large numbers of SNe Ia at $0.05 \lesssim z \lesssim 0.35$. The survey is designed to take advantage of the extensive database of reference images, object catalogs, and photometric calibration previously obtained by the SDSS-I. The uniformity of the SDSS 2.5 m photometric instrumentation, in conjunction with *in situ* photometric standards *from the same telescope*, minimizes systematic errors arising from instrumental color terms and multi-stage transfer of photometric standards. By the time it is completed, the SDSS-II Supernova Survey will increase the

number of "fully characterized" SN Ia light curves (with multicolor data before peak and densely-sampled, well-calibrated light curves) by a significant factor.

This paper serves as an overview of the SDSS-II Supernova Survey. The scientific motivation and survey goals are discussed in Section 2. The observational strategy is briefly described in Section 3, and Section 4 overviews the data processing and target selection for the program. In Section 5 we describe the spectroscopic follow-up program, and we conclude in Section 6. Throughout, we highlight some of the results from the first two seasons of observations. This paper serves as a companion and introduction to more detailed papers describing the methods and results from the first observation season. A detailed technical discussion of the on-mountain data processing and spectroscopic selection algorithm is presented by Sako et al. (2007). Holtzman et al. (2007) describe the algorithm used to obtain SN photometry and present the photometry from the 2005 season. Zheng et al. (2007) describe the corresponding SN spectroscopy. Dilday et al. (2007) present the measurement of the SN Ia rate at low redshift from the 2005 season. Phillips et al. (2007) and Prieto et al. (2007) present data on the peculiar SNe 2005hk and 2005gj. Becker et al. (2007, in preparation) describe the discovery of trans-Neptunian objects with these data.

2. SCIENTIFIC GOALS

The SDSS-II Supernova Survey aims to address the following primary science goals.

1. *Cosmological parameters from the SN Ia Hubble diagram.* Measurements of SN Ia distances constrain the history of the Hubble expansion parameter. For illustration, assuming a spatially flat Universe and constant dark energy equation of state parameter w (the ratio of its effective pressure to its energy density), the luminosity distance satisfies $d_L = [(1+z)/H_0] \int dz'/[\Omega_m(1+z')^3 + (1-\Omega_m)(1+z')^{3(1+w)}]^{1/2}$, where Ω_m is the fractional density in non-relativistic matter. The SDSS-II SN Survey will obtain distance modulus estimates for $\sim$100 well-measured SNe Ia in each of the three $\Delta z = 0.1$ bins spanning the redshift range $0.05 < z < 0.35$. Occupying a hitherto sparsely populated region of the Hubble diagram, these data will provide important information on the evolution of the cosmic scale factor that is not accessible to any current supernova survey. Assuming that the intrinsic SN Ia distance modulus dispersion is

0.15 mag (in the *V* band, Phillips et al. 1999), the SDSS-II SN Survey will determine the mean distance modulus with a *statistical* uncertainty of ~0.015 mag per redshift bin. At redshift $z = 0.2$, that uncertainty is less than the difference in distance modulus between two cosmological models differing by $\delta w = 0.1$ (with all other cosmological parameters fixed). In combination with higher-redshift SN samples from ESSENCE (Miknaitis et al. 2007; Wood-Vasey et al. 2007) and Supernova Legacy Survey (SNLS) (Astier et al. 2006), and with other cosmological probes that primarily constrain the matter density Ω_m (e.g., baryon acoustic oscillations, Eisenstein et al. 2005), the SDSS-II SN Survey will lead to more robust cosmological constraints. The intermediate-redshift range probed by the SDSS-II SN Survey is also of interest because, if $w \simeq -1$, as suggested by current data, dark energy began dominating over non-relativistic matter at $z \approx 0.4$.

2. *Minimization and evaluation of SN systematics.* Systematic errors are comparable to statistical errors in the SN surveys that have reported recent results; for future SN cosmology studies with larger datasets, improved control of systematic errors will be essential. The systematics arising from photometric calibration errors are small for the SDSS: years of effort on the large-scale calibration of the imaging data (Smith et al. 2002) have achieved 1% photometric errors over the area of the SDSS-II SN Survey (Ïvezić et al. 2007). The SDSS-II SN observations employ five filters, providing substantial color information, especially for the low-redshift portion of the sample. It uses a single, stable camera system with well-calibrated and repeatedly measured filter transmission curves, and the SDSS native magnitudes (which are used throughout this paper) are close to the physical AB system (Oke & Gunn 1983), with well-measured offsets. The large number of SDSS SN light curves can be partitioned into subsets at common redshift to investigate potential sources of systematic error that may afflict SN Ia distance measurements, as well as to search for correlations between Hubble diagram residuals and host-galaxy morphology, metallicity, or extinction.

3. *Anchoring the Hubble diagram and light-curve training.* When completed, the low-redshift portion of the SDSS-II SN sample ($z \lesssim 0.15$) will be large enough and of sufficiently high data quality to anchor the Hubble diagram and to re-train light-curve fitters, reducing or eliminating reliance on the heterogeneous low-redshift samples currently employed. The low-redshift portion of the SDSS sample is also distant enough that the effects of correlated peculiar velocities due to large-scale flows (Radburn-Smith et al. 2004; Hui & Greene 2006; Cooray & Caldwell 2006), which may be a non-negligible source of systematic error in existing lower-redshift samples—e.g., the "Hubble bubble" (Zehavi, et al. 1998; Jha et al. 2007; Conley et al. 2007)—are small compared to the statistical errors. The large sample and high quality of supernova light curves will provide an unprecedented opportunity to study in detail the color/peak brightness/decline-rate relationship, and to search for any additional photometric parameters that may further reduce the scatter in the Hubble diagram.

4. *Rest-frame ultraviolet light-curve templates for high-z SN surveys.* SN surveys that extend to $z \gtrsim 1.5$ will be required to achieve robust constraints from supernovae on the time evolution of the dark energy equation of state (e.g., Frieman et al. 2003), as envisioned in the concepts proposed for the NASA-DOE Joint Dark Energy Mission. *Hubble Space Telescope* pilot programs in the $z > 1$ regime are in progress (Riess et al. 2007; Barbary et al. 2006). To reduce systematic errors, these high-redshift SN light curves must be matched to a set of low-redshift templates. For example, at $z = 1.2$, observations in the reddest optical passbands, ~8000 Å, correspond to 3600 Å, i.e., the *u* band, in the SN rest frame. The SDSS SNe observed at $z = 0.3$ will have this spectral region observed at 4700 Å, covered by the SDSS *g* band; the survey will thus improve the rest-frame ultraviolet template data (Jha et al. 2006; Wang et al. 2005) needed for the interpretation of high-redshift SNe.

5. *SN cosmology from multi-band photometry.* Future wide-field imaging surveys, such as Dark Energy Survey (DES) (Abbott et al. 2005), PanSTARRS (Kaiser 2002), and Large Synoptic Survey Telescope (LSST) (Tyson 2002), will measure optical, multi-band light curves for thousands to hundreds of thousands of supernovae. Spectra, which have been traditionally used to determine SN types and redshifts, will be obtainable for only a small fraction of them. As they evolve, SNe Ia trace out a distinct locus in multi-color and light-curve shape space which, along with host-galaxy colors, provides information on SN type, redshift, and age (Poznanski et al. 2002; Vanden Berk et al. 2001; Johnson & Crotts 2006; Sullivan et al. 2006a; Sako et al. 2007). Future surveys will rely heavily on the ability to use this information to *photometrically* determine SN type and redshift. With its large database of multi-band SN photometry and follow-up spectroscopy, the SDSS SN Survey will provide an excellent testing ground for development of this technique.

6. *SN rates, host galaxies, and rare SN types.* In addition to the spectroscopically confirmed SNe Ia, the survey yields light curves for a multitude of additional supernovae: objects that are almost certainly SNe Ia but which we were unable to confirm spectroscopically, as well as other types of supernovae. Combined with careful monitoring of the detection efficiency using artificial SNe inserted into the data stream, this large photometric SN sample will enable robust measurement of SN rates.

The process in which a white dwarf explodes as a SN Ia remains a mystery, since the progenitors are so faint that no extragalactic event can be directly observed before exploding. The large SDSS supernova sample provides an unbiased census of host galaxies whose stellar ages and metal abundances are clues to the progenitor properties (e.g., Gallagher et al. 2005; Sullivan et al. 2006b). Stellar population and metallicity evolution are important systematic uncertainties in measuring dark energy with supernovae, and their effect on SN Ia luminosity can be constrained with the study of a large host-galaxy sample.

The SDSS-II SN Survey will also produce a homogeneous set of core-collapse SN light curves, a small fraction of which will be spectroscopically identified; there is evidence that SNe II may also prove to be useful cosmological probes (e.g., Hamuy & Pinto 2002; Baron et al. 2004).

Finally, since it covers a larger volume than previous or other current SN surveys, the SDSS also probes rare but intrinsically interesting objects such as "broad-line" Type Ib/c supernovae (some of which appear to be associated with GRBs; see Woosley & Bloom 2006 for a review) and

peculiar SNe Ia (e.g., Li et al. 2001, 2003; Hamuy et al. 2003; Chornock et al. 2006; Phillips et al. 2007; Aldering et al. 2006; Prieto et al. 2007).

3. OBSERVING STRATEGY

The SDSS-II SN Survey primary instrument is the SDSS CCD camera (Gunn et al. 1998) mounted on a dedicated 2.5 m telescope (Gunn et al. 2006) at Apache Point Observatory, New Mexico. The camera obtains, nearly simultaneously, images in five broad optical bands (*ugriz*; Fukugita et al. 1996). The camera is used in time-delay-and-integrate (TDI, or drift scan) mode, which provides efficient sky coverage. The Supernova Survey scans at the normal (sidereal) SDSS survey rate, which yields 55-s integrated exposures in each passband; the instrument covers the sky at a rate of approximately 20 sq. deg h^{-1} and achieves 50% detection completeness for stellar sources at $u = 22.5$, $g = 23.2$, $r = 22.6$, $i = 21.9$, and $z = 20.8$ (Abazajian et al. 2003). For comparison, the typical peak magnitude for a SN Ia with no extinction is $r \simeq 19.3$, 20.8, and 21.6 mag for $z = 0.1$, 0.2, and 0.3.

The SDSS-II SN Survey scans a region (designated stripe 82) centered on the celestial equator in the southern Galactic hemisphere that is 2.5° wide and runs between right ascensions of 20^h and 4^h, covering a total area of 300 sq. deg. Since there are gaps between the six CCD columns in the focal plane, this area is typically covered by alternating, on successive nights of observation, between the interleaving northern and southern declination strips of the stripe. In addition to being nearly optimal for finding SNe Ia in the redshift desert, sidereal scanning benefits from many years of SDSS survey operations and data processing experience. Except near its ends, the stripe 82 area has low Galactic extinction (Schlegel et al. 1998), can be observed from Apache Point at low airmass from September through November, and is accessible from almost all ground-based telescopes for subsequent spectroscopic and photometric observations. This stripe has two important additional features, arising from the fact that it has been imaged numerous times during the SDSS-I survey (2000–5) in photometric conditions with good seeing ($<1.5''$). First, the resulting deeper, co-added images, with a median of ten single-epoch exposures per band, provide a high-quality, photometrically calibrated template for carrying out image subtraction to discover supernovae. Second, the repeated imaging has enabled improved photometric calibration at the ~1% level (Ĭvezić et al. 2007).

During the period 2005–7 September 1 through November 30, the Supernova Survey is carried out on most of the useable observing nights. The exceptions are the five brightest nights around each full moon, nights used for telescope engineering (which generally bracket the five full-moon nights), and occasional nights used by the SDSS-II SEGUE project. Accounting for weather, the Moon, and the interrupts above, each region in the survey area has been imaged on average every five nights during the first two seasons, while the average on-sky cadence during non-bright time is about every 4.5 nights, as shown in Figure 1. As a rolling survey with high cadence, SDSS SN is able to find supernovae well before maximum light (for $z \lesssim 0.3$); Figure 2 shows that the vast majority of spectroscopically confirmed SNe Ia were discovered before peak light. The discovery epochs shown here are from the on-mountain search photometry; in some cases, final photometric reductions reveal detections at even earlier epochs. The curve in the figure shows the expected epoch at which a typical SN Ia at that redshift reaches $r = 22.5$. This does not
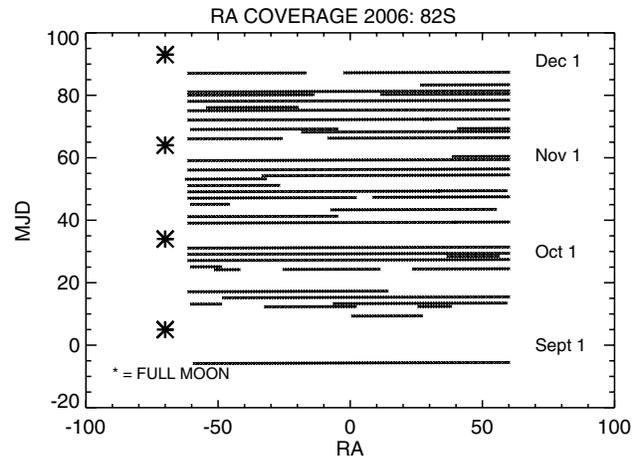
Figure 1. Right ascension coverage (in degrees) versus time (measured from September 1, i.e., MJD-53980) for the southern half of stripe 82 during the 2006 SDSS SN season. The large asterisks denote gaps around full moon. The first scan was taken in late August to minimize survey edge effects. The first part of 2006 September suffered from poor observing conditions.
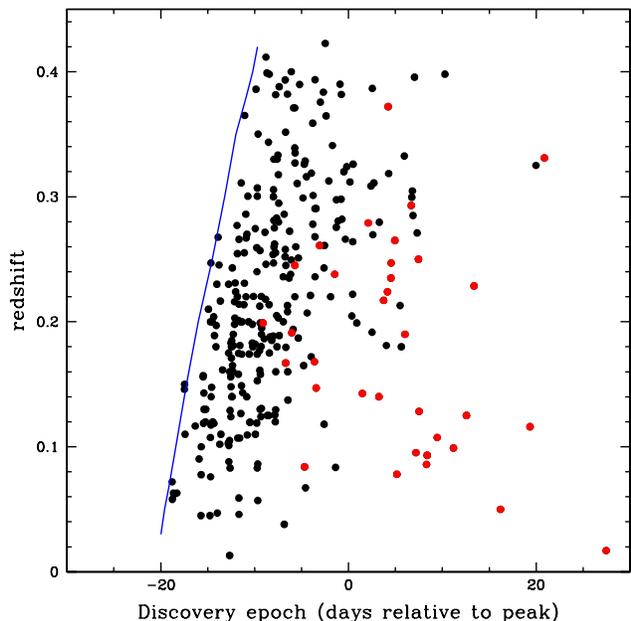
Figure 2. Photometric discovery epoch relative to estimated time of *g*-band peak light versus redshift, for 312 spectroscopically confirmed SNe Ia from the 2005 and 2006 seasons. The epoch of peak light is determined from light-curve fits to the on-mountain photometry. Open points denote supernovae that reached peak light at least seven days after the start of the survey on September 1; filled points denote supernovae that peaked before September 7 and account for most of the SNe found after peak. The solid curve shows the expected epoch at which a fiducial model SN Ia, with decline-rate parameter $\Delta m_{15} = 1.2$ and no extinction, reaches $r = 22.5$.

(A color version of this figure is available in the online journal)

imply that this is our photometric limit, but it does indicate that the left-hand boundary of the locus of points in the figure is due primarily to the flux limit of the survey. The high survey cadence and detection limit result in well-sampled, multi-band light curves, as shown, e.g., in Figure 3 (see also Holtzman et al. 2007). Since SNe Ia typically spend about 25 rest-frame days brighter than 1 mag below peak light, the three-month annual survey duration is long enough that the efficiency hit due to survey "edge effects" (in time) is acceptable. For 2006,
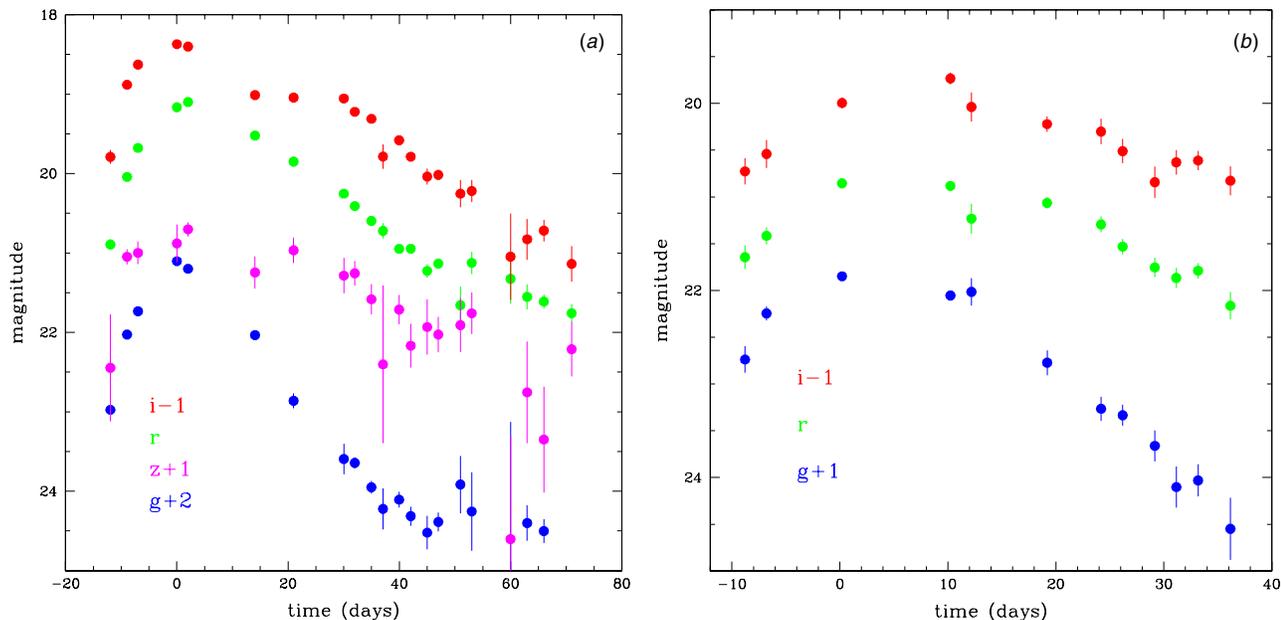
Figure 3. Left: *griz* light curves for SN 2005ff, a confirmed SN Ia at $z = 0.088$; this light curve is particularly well sampled because it lies in the region where the northern and southern halves of stripe 82 overlap. Right: *gri* light curves for SN 2005gg, a confirmed SN Ia at $z = 0.231$. Time is measured in days from the peak of *g*-band light.

(A color version of this figure is available in the online journal)

about 76% of the confirmed SNe Ia reached peak light at least one week after the observing season started and at least ten days before it ended. This efficiency can be controlled by preferentially targeting for spectroscopy those objects which have high probability of yielding well-sampled light curves. The inefficiency can be further minimized by carrying out targeted photometric follow-up observations of SNe on other telescopes into December (see Section 5).

4. DATA PROCESSING AND TARGET SELECTION

We use a dedicated computer cluster at the observatory to perform rapid reductions of the SDSS-II SN imaging data (see Sako et al. (2007) for more details). The *ugriz* data are processed through the first stages of the standard SDSS photometric reduction pipeline (Lupton et al. 2001) to produce "corrected," astrometrically calibrated (Pier et al. 2003) images for the SN search data. The deeper co-added reference images, comprising data taken up through 2004, are convolved to match the point-spread functions of the search frames and subtracted from them, using a modified version of the frame subtraction pipeline developed for ESSENCE (Miknaitis et al. 2007). "Real-time" image subtraction is limited to the *gri* bands, which are the bands most useful for SN detection in the redshift range of interest. The subtracted images are processed through an automated object detection algorithm, which yields initial photometric measurements. Objects detected in more than one passband that are not coincident with previously catalogued stars or variable objects and not detected as moving during the ∼5 min interval between the *g* and *r* exposures are selected for further study. For a full night of imaging, this processing is generally completed within 24 h or less, and the resulting object information is sent electronically to a computer at Fermilab.

For the Fall 2005 observing season, image cutouts of all objects passing the above criteria were manually evaluated us-

ing a web interface. For 2006, additional and improved software cuts were applied to reduce the number of objects visually scanned without sacrificing discovery potential. In 2006, single-epoch detections were only passed to manual scanning if they were not detected as moving (with an improved "autoscanner" algorithm for vetoing moving objects; see Sako et al. 2007) and if they were bright, with either $r < 21$ or $g < 21$. Otherwise, at least two detection epochs were required for an object to be scanned. Visual screening is mainly intended to reject artifacts and other objects that are obviously not supernovae; artificial supernovae inserted into the images are used to monitor the efficiency of this process. Objects that pass this screening are denoted "candidates." Subsequent object detections at the same position are automatically added to the database of information about each candidate. In 2005, approximately 6753 sq. deg. of imaging data were processed on the mountain; 145,395 objects were manually scanned, yielding 11,385 unique SN candidates and 130 spectroscopically confirmed SNe Ia. The majority of objects scanned were single-epoch subtraction artifacts, low signal-to-noise fluctuations, and moving objects; the majority of the resulting SN candidates were astrophysical transients, including moving objects, unvetoed variable stars, and active galactic nuclei (AGN). In 2006, approximately 7354 sq. deg. of data were processed; with the pipeline improvements described above, only 14,404 objects were scanned, yielding 3694 candidates and 197 spectroscopically confirmed SNe Ia.[48]

---

[48] The viability of detecting and following SNe from SDSS imaging data was demonstrated in earlier pilot runs. In Fall 2002, 77 SN candidates were detected in several SDSS scans on stripe 82; 39 of them were subjected to subsequent spectroscopic observation, resulting in 18 confirmed SNe Ia out to $z \simeq 0.4$ and 8 SNe of other types (Miknaitis et al. 2002). In Fall 2004, an engineering test run for the SDSS-II SN Survey was carried out using 20 nights scheduled over 1.5 months, yielding 16 spectroscopically confirmed SNe Ia, 5 SNe II, and 1 SN Ib/c (Sako et al. 2005).

The *gri* light curve for each SN candidate is fit with templates for different SN types and redshifts, allowing for variable reddening and, for SNe Ia, variable light-curve stretch. If host-galaxy spectroscopic or photometric redshift information is available from the SDSS database, it can also be included in the fit. As data on a candidate accumulate over time, the fits are updated. Based on relative χ^2 values, SN Ia-like light curves are identified, and a large subset of them are targeted for spectroscopy to determine redshift and confirm SN type. All SN Ia candidates found before peak and with estimated current *r*-band magnitude $\lesssim 20$ are placed on the target list; they are generally accessible with 3–4 m class telescopes, so our follow-up observations are nearly complete out to that magnitude. There is a much larger number of fainter, higher-redshift candidates for which the follow-up resources are limited; those are prioritized based on good light-curve coverage, low estimated host-galaxy light contamination, and low host-galaxy dust extinction estimated from the light-curve fits. The basic goal is to target those SNe for which we expect to achieve accurate distance estimates based on the SDSS photometry. For details of the target selection algorithm, see Sako et al. (2007).

Final SN photometry is carried out after each season using the "scene-modeling" code developed for the SDSS-II SN Survey (Holtzman et al. 2007). This approach is similar in spirit to the algorithm used by SNLS (Fabbro 2001, Astier et al. 2006), except that it involves no pixel re-sampling, so that error propagation can be properly handled at the pixel level. A sequence of stars around each SN is taken from the list of Ivezić et al. (2007), who derived standard magnitudes from multiple observations taken during the main SDSS survey under photometric, good seeing conditions. Using these stars, frame scalings and astrometric solutions are derived for each of the SN frames, as well as for pre-supernova frames on stripe 82 taken as part of either the main SDSS survey (pre-2005) or the SN survey. Finally, the entire stack of frames is simultaneously fit for a single supernova position, a fixed galaxy background in each filter (characterized by a grid of galaxy intensities), and the supernova brightness in each frame. Final photometry is carried out in all five SDSS passbands; however, since SNe Ia are intrinsically UV-faint and the SDSS system throughput is low in the *z* band, we typically detect SNe Ia in the *u* and *z* bands only at modest redshift, $z \lesssim 0.15$. Figure 3 shows light curves for two SNe Ia based on the outputs of the scene-modeling photometry code.

Figure 4 shows the approximate distribution of the number of SDSS photometry epochs for the spectroscopically confirmed SNe from the first two seasons for all types (in black) and for SNe Ia (in red). An epoch here constitutes a detection in at least two of the *gri* bands; in the majority of cases, the SN is detected in all three bands. The median number of photometric epochs per supernova is 9 based on the on-mountain photometric detections. The final scene-modeling photometry often produces detections at additional epochs at faint flux levels, and additional photometric epochs observed with other telescopes are available for a subset of the supernovae (see discussion at the end of Section 5).

All spectroscopically confirmed supernovae are announced in a timely manner through the Central Bureau for Electronic Telegrams. In addition, bright (i.e., low-redshift) SN candidates observed for at least two epochs and found on the rise are announced, often before spectroscopic confirmation. Moreover, as of the 2006 season, all candidates, with all relevant photometric
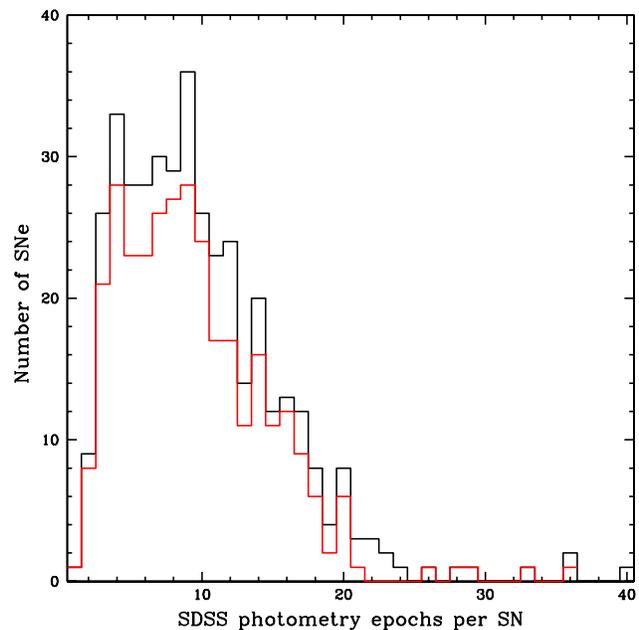
Figure 4. Distribution of number of SDSS photometry epochs for confirmed SNe of all types (dashed) and for SNe Ia (solid) for the 2005 and 2006 seasons, based on the on-mountain photometric reductions.

(A color version of this figure is available in the online journal)

information (based on the on-mountain reductions), are made available on the worldwide web as soon as they are identified.[49] In collaboration with VOEventNet (Drake et al. 2006), as of 2006 we are also sending all candidates verified by a second epoch of observation to a publicly accessible messaging system, regardless of the results of our light-curve fits to supernova templates. By using this rapid messaging system and standard communication packets structured as XML-format VOEvents, in principle we enable nearly instantaneous follow-up observations of our candidates by a global network of telescopes subscribing to the VOEventNet feed. In 2006, we released information on 3075 two-epoch candidate events,[50] and we expect to generate a similar number of events during the 2007 season. Finally, the corrected images and photometric catalogs for all the SN data are made available to the community soon after they are reprocessed through the SDSS photometric pipeline at Fermilab.[51]

5. FOLLOW-UP OBSERVATIONS: SPECTROSCOPY AND PHOTOMETRY

Spectroscopy of SN candidates is carried out on a number of telescopes, primarily to determine SN type and redshift but also to measure other properties. Where possible, a host-galaxy spectrum is extracted as well, enabling more accurate redshift determination from the narrower galaxy spectral features and determination of host-galaxy spectroscopic type. For our sample, the redshifts based on host-galaxy features are accurate to about $\Delta z = 0.0005$, while those based on SN Ia features are accurate to about $\Delta z = 0.005$. For approximately two-thirds of the confirmed SNe Ia, we have redshifts determined from host-galaxy features.

---

[49] http://sdssdp47.fnal.gov/sdsssn/sdsssn.html.
[50] http://voeventnet.caltech.edu/SDSS.shtml.
[51] http://www.sdss.org/drsn1/DRSN1_data_release.html.
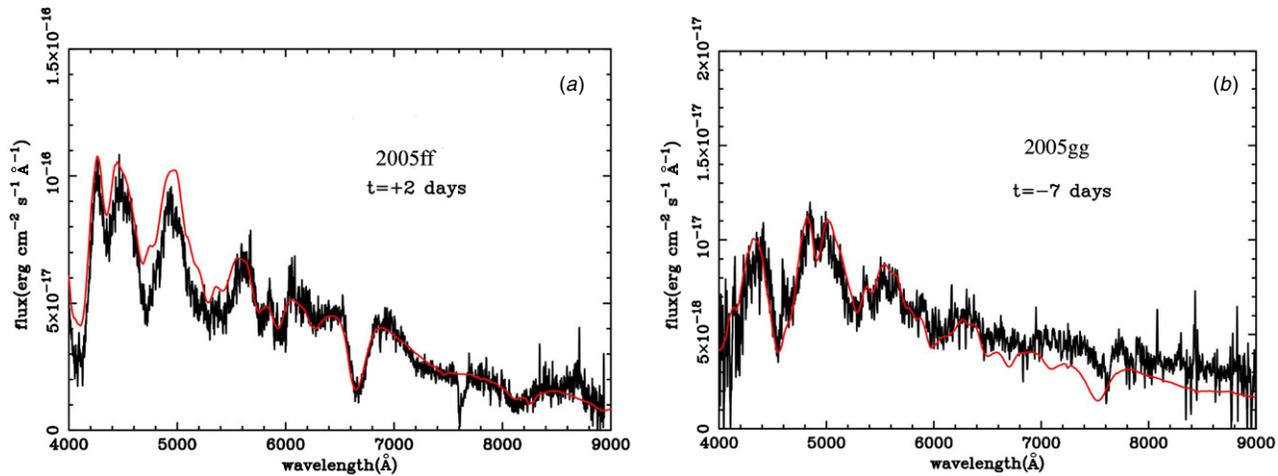
Figure 5. Spectra of the SNe Ia shown in Figure 3. Left: WHT spectrum of SN 2005ff; Right: Subaru spectrum of SN 2005gg. Galaxy light has not been subtracted. Solid curves denote template SN Ia spectra at the indicated epochs relative to peak light. The abscissa shows observed wavelength.

(A color version of this figure is available in the online journal)

Table 1
Telescope Resources Allocated for Spectroscopic Observations in 2005 and 2006

Telescope	Aperture (m)	Nights scheduled	SNe observed
HET	9.2	64.5 h (2005)	66
		80 h (2006)	77
NTT	3.6	17 (2006)	70
ARC	3.5	31 Half-nights (2005)	47
		28 Half-nights (2006)	31
Subaru	8.2	6 Shared (2005)	33
		4 (2006)	33
MDM	2.4	49 Shared (2005)	27
		50 Shared (2006)	26
WHT	4.2	6 (2005)	26
KPNO	4	6 (2006)	15
Keck	10	1 ToO (2005)	14
		1 ToO (2006)	4
NOT	2.6	4 (2006)	10
SALT	11	ToO (2006)	5

Notes. Actual time used is less due to weather and instrument problems. Shown are the amounts allocated for September–December. Target of opportunity (ToO) denotes time that was not specifically scheduled for SDSS SN observations. The HET and SALT are queue-scheduled. A portion of the MDM and ARC time allocation listed here was used for additional photometric observations. The last column includes multiple observations of the same SN and includes all confirmed SN types. Legend (for more information, see acknowledgements at the end of the paper): HET: Hobby–Eberly Telescope, McDonald Observatory, Texas; NTT: ESO New Technology Telescope, La Silla Observatory, Chile; ARC: Apache Point Observatory 3.5 m telescope, New Mexico; Subaru: Subaru Telescope, National Astronomical Observatory of Japan, Hawaii; MDM: Hiltner Telescope, MDM Observatory, Arizona; WHT: William Herschel Telescope, La Palma; KPNO: Kitt Peak National Observatory, Arizona; Keck: W. M. Keck Observatory, Hawaii; NOT: Nordic Optical Telescope, La Palma; SALT: South African Large Telescope, South African Astronomical Observatory.

Table 1 lists the spectroscopic resources, the amount of time scheduled on them for each of the first two seasons, and the number of SNe observed. In addition to those listed in Table 1, in a handful of cases spectra have been taken by other observers/telescopes based on information we have released in electronic circulars or through informal communication. These include the Center for Astrophysics group (S. Blondin, M. Modjaz, R. Kirshner, P. Challis, M. Hicken, M. Calkins, and

L. Macri), the Nearby Supernova Factory, and the ESSENCE team.

Spectra are analyzed (Zheng et al. 2007) to determine SN type, and the redshift is determined from either the SN or host-galaxy spectrum (or both) using standard cross-correlation techniques. Spectra that are consistent with those of SNe Ia but for which the identification is not highly confident are denoted probable SNe Ia. Two spectra from the 2005 season are shown in Figure 5.

The early light-curve fitting and target selection algorithm described above in Section 4 has proven to be very efficient at photometrically identifying SNe Ia. Approximately 90% of the objects targeted as SN Ia candidates after two or more epochs of photometry indeed turned out to be SNe Ia; about 86% of the targets were spectroscopically confirmed, while the other 4% have high signal-to-noise, multi-band light curves that leave no doubt that they are SNe Ia. The remaining spectra (about 10%) are mostly unclassifiable, often as a result of marginal observing conditions, but also include a very small percentage of AGN and core-collapse SNe ($\sim$2%). In addition to SNe Ia, we have also targeted a sample of bright ($r < 20$ mag) core-collapse SN candidates. Although the colors of these events could be confused with those of an AGN, we generally avoid candidates that appear within $\sim$0.5″ of the host-galaxy nucleus. The confirmation efficiency for these events is $\sim$90%, comparable to that of the SNe Ia.

Figure 6 shows the redshift distributions for the spectroscopically confirmed SNe Ia from the 2005 (black) and 2006 (red) seasons. For 2005, there were 130 spectroscopically confirmed and 16 spectroscopically probable SNe Ia; for 2006, the corresponding numbers were 197 and 14. The major difference between the two seasons is the large increase in the spectroscopic yield in the redshift range $0.12 < z < 0.24$; this is attributable to changes in targeting strategy (we placed less emphasis on the highest-redshift candidates in 2006) and to the large increase in 3–4 m telescope resources for spectroscopy, as shown in Table 1. The blue histogram shows the 2005 confirmed SN Ia sample augmented by a set of 94 host-galaxy redshifts for objects with SN Ia-like light curves (see below), and the magenta histogram shows the redshift distribution for the combined sample of 421 SNe Ia to date. The mean redshift for the combined sample is $z = 0.22$.
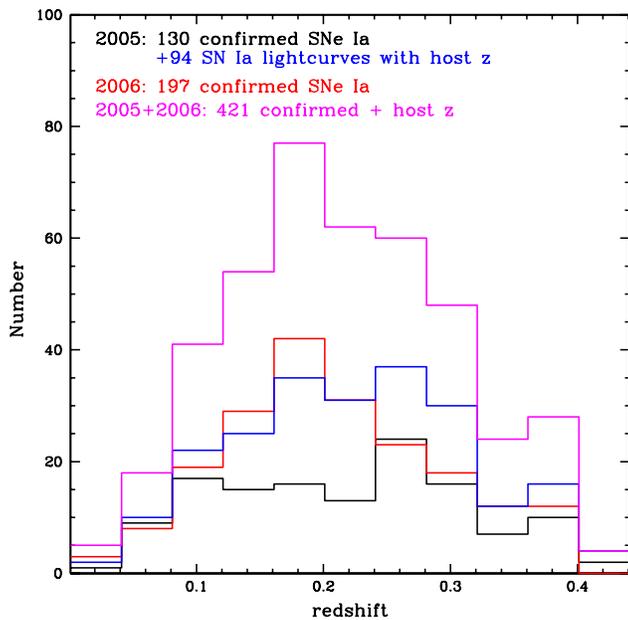
Figure 6. Histogram of redshifts of spectroscopically confirmed SNe Ia for the 2005 (short-dashed) and 2006 (dotted) seasons. Long-dashed histogram shows the 2005 confirmed sample plus 94 objects with SN Ia light curves and subsequent host-galaxy redshift measurements. The solid histogram shows the sum of these three distributions.

(A color version of this figure is available in the online journal)

Figure 7. Distribution of epoch relative to g-band peak light of first spectroscopic observations for the spectroscopically confirmed SNe Ia from the 2005 and 2006 seasons. The epoch of peak light is estimated from light-curve fits to the on-mountain photometry.

Figure 7 shows the distribution of the epoch of first spectroscopic observation relative to peak light in the g band for the spectroscopically confirmed SNe Ia from 2005 and 2006, where the latter is determined from light-curve fits to the on-mountain photometry (Sako et al. 2007). Two-thirds of the first-epoch spectra were taken within ±10 days of peak light, when a SN Ia is within roughly 1 mag of maximum, and 28% were taken before peak light.

Since spectroscopic resources are limited, we cannot target all SN Ia candidates, even all those with good-quality light curves: targets listed at low priority may not make it onto the queue of any of the telescopes or may not be observed before fading, due to poor weather, etc. To gauge the resulting completeness, after each season we reprocess a large subset of the SN candidates. For the 2005 season, to find additional SNe Ia, we first selected all photometric SN candidates detected at two or more epochs by the on-mountain photometry pipeline. Those for which the best-fit light-curve template was a SN Ia were processed through the final scene-modeling photometry pipeline; in many cases, additional detection epochs were thereby recovered. For candidates with resulting high-quality SN Ia-like light curves which had not been spectroscopically confirmed, we carry out host-galaxy spectroscopy, as resources permit, to determine the redshift and measure host-galaxy properties. To date, we have obtained host spectra and redshifts for 81 such photometric SN Ia candidates from the 2005 season, primarily with HET. An additional 13 photometric SN Ia candidates have host spectra from the SDSS redshift survey. The redshift distribution for this combined photometric sample, added to the spectroscopically confirmed 2005 supernovae, is shown as the blue histogram in Figure 6. We see that these objects largely fill in the gap at $z \simeq 0.2$ in the 2005 spectroscopic sample.

The distribution in RA and redshift for the spectroscopically confirmed SNe Ia is shown in Figure 8. The SNe Ia are shown
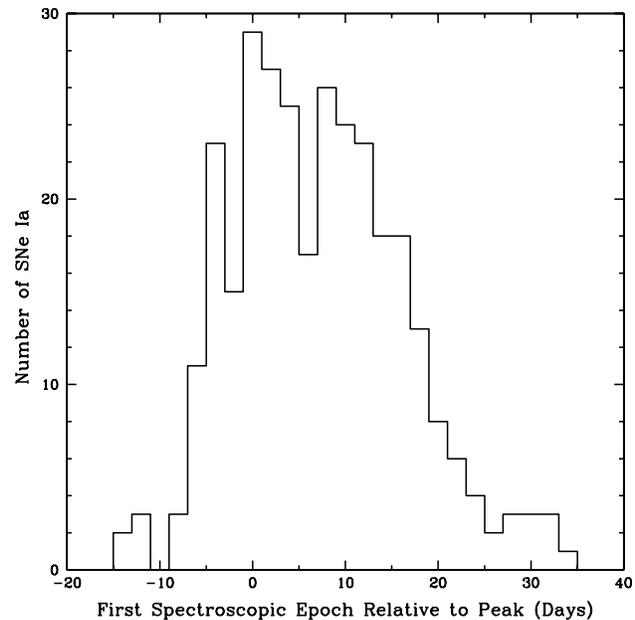
(large purple points) superposed on the distribution of galaxies with measured redshifts from the SDSS (black and red points, with color indicating whether the galaxy is at positive or negative declination within stripe 82).

A subsample of the confirmed SNe are targeted for several or more epochs of spectroscopy. These include peculiar or otherwise interesting SNe Ia, e.g., SN 2005hk (Phillips et al. 2007) and SN 2005gj (Prieto et al. 2007), for which spectral evolution can inform physical modeling. In addition, normal SNe Ia with several epochs of spectroscopy will be used to explore development of improved K-correction models and to study correlations between spectroscopic evolution and photometric properties. Figure 9 shows the number of spectroscopic epochs obtained for all spectroscopically confirmed SNe (of all types) as a function of redshift.

In addition to SDSS photometry and follow-up spectroscopy, a number of SDSS SNe have been imaged in SDSS filters and in other passbands with other telescopes. These additional photometric data are taken for a variety of reasons: to provide more rapid confirmation of SNe at early epochs, to fill in SDSS light curves during periods of bad weather at APO, and to extend light curves for SNe that have faded beyond the SDSS detection limit or that are still near peak light at the end of the SDSS observing season on November 30. Telescopes used for this purpose include the University of Hawaii 2.2 m, the Hiltner 2.4 m at MDM, the New Mexico State University 1 m at APO, the ARC 3.5 m, the 1.8 m Vatican Advanced Technology Telescope at Mt. Graham, the 3.5 m WIYN telescope at Kitt Peak, the 1.5 m optical telescope at Maidanak Observatory in Uzbekistan, and the 2.5 m Isaac Newton Telescope at La Palma. For 2005 and 2006, 177 confirmed SNe were imaged at least once by one of these telescopes. In addition, the Carnegie Supernova Project is obtaining densely-sampled optical and near-infrared (NIR) imaging for many of the SDSS SNe at $z < 0.08$ and NIR imaging near peak for a subsample of SDSS SNe at $z \simeq 0.3$. Given
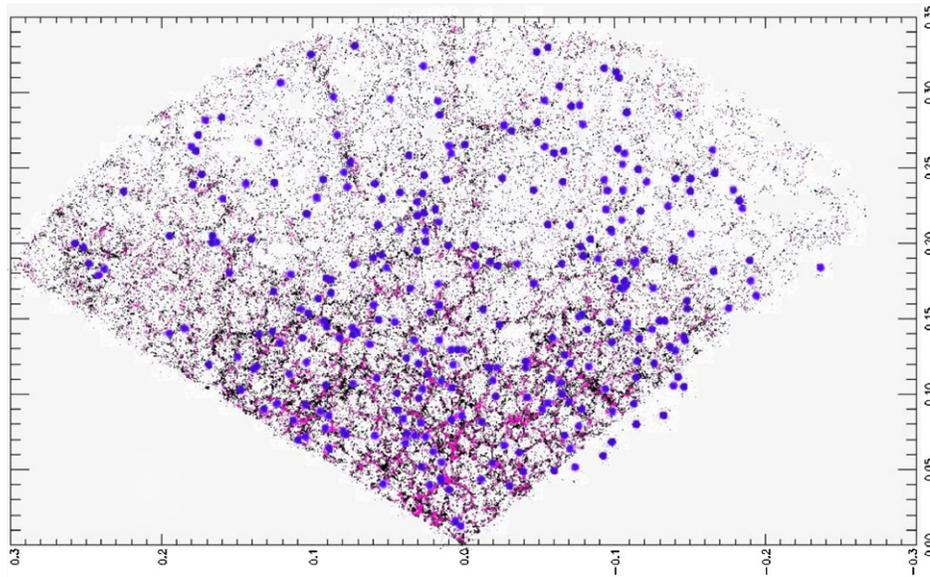
Figure 8. Distribution of confirmed SDSS-II SNe Ia from 2005 and 2006 in RA and redshift (large points), superposed on the distribution of galaxies with redshifts measured by the SDSS (small points). The SN survey extends slightly beyond the RA limits for the redshift survey, leading to the handful of SNe that appear "out of bounds."

(A color version of this figure is available in the online journal)
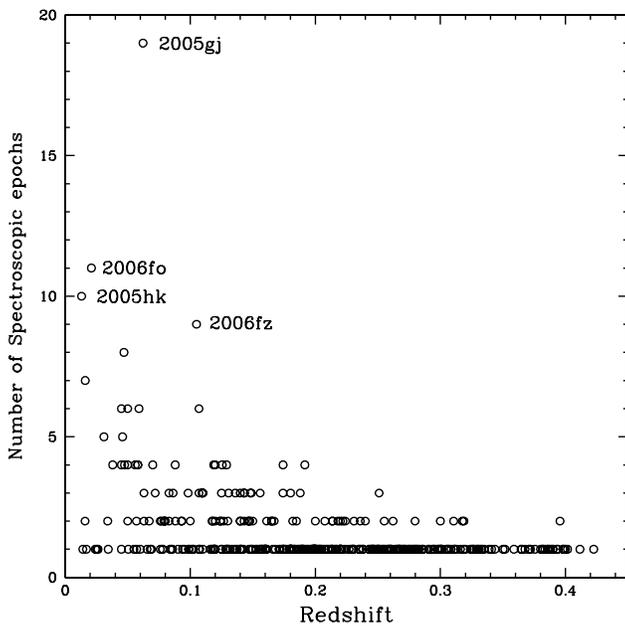
Figure 9. Number of spectroscopic epochs per supernova versus redshift for confirmed SNe from the 2005 and 2006 seasons. IAU designations for those with the most epochs of spectroscopy are indicated.

the differences in filter response for this variety of instruments, careful attention to color terms and calibrations is necessary to combine these data with SDSS photometry (see Holtzman et al. 2007).

6. CONCLUSION

The SDSS-II Supernova Survey has completed the first two of its planned three three-month observing seasons. Light curves have been measured for 327 spectroscopically confirmed SNe Ia.

Including spectroscopically probable SNe Ia, other confirmed SN types, and objects with SN Ia-like light curves and host-galaxy spectroscopy, the yield to date is 496. The Fall 2007 season should increase the sample size by about 50%.

REFERENCES

Abazajian, K., et al. 2003, AJ, 126, 2081
Abbott, T., et al. (DES Collaboration) 2005, arXiv astro-ph/0510346
Aldering, G., et al. 2006, ApJ, 650, 510
Astier, P., et al. 2006, A&A, 447, 31
Barbary, K., et al. 2006, AAS Abstr., 209, 90.01
Baron, E., et al. 2004, ApJ, 616, L91
Chornock, R., Filippenko, A. V., Branch, D., Foley, R. J., Jha, S., & Li, W. 2006, PASP, 118, 722
Conley, A., Carlberg, R. G., Guy, J., Howell, D. A., Jha, S., Riess, A. G., & Sullivan, M. 2007, ApJ, 664, L13
Cooray, A., & Caldwell, R. R. 2006, Phys. Rev. D, 73, 103002
Dilday, B., et al. 2007, ApJ, submitted
Drake, A. J., et al. 2006, BAAS, 209, 7804
Eisenstein, D., et al. 2005, ApJ, 633, 560
Fabbro, S. 2001, PhD thesis, Université Denis Diderot, Paris
Filippenko, A. V. 2005, in White Dwarfs: Cosmological and Galactic Probes, ed. E. M. Sion, S. Vennes, & H. L. Shipman (Dordrecht: Springer), 97
Frieman, J. A., Huterer, D., Linder, E. V., & Turner, M. S. 2003, Phys. Rev. D, 67, 083505
Fukugita, M., Ichikawa, T., Gunn, J. E., Doi, M., Shimasaku, K., & Schneider, D. P. 1996, AJ, 111, 1748
Gallagher, J. S., Garnavich, P. M., Berlind, P., Challis, P., Jha, S., & Kirshner, R. P. 2005, ApJ, 634, 210
Gunn, J. E., et al. 1998, AJ, 116, 3040
Gunn, J. E., et al. 2006, AJ, 131, 2332
Hamuy, M., et al. 2003, Nature, 424, 651
Hamuy, M., & Pinto, P. 2002, ApJ, 566, L63
Holtzman, J., et al. 2007, AJ, submitted
Hui, L., & Greene, P. 2006, Phys Rev D, 73, 123526
Ívezić, Z., et al. 2007, AJ, 134, 973
Jha, S., et al. 2006, AJ, 131, 527
Jha, S., Riess, A. G., & Kirshner, R. P. 2007, ApJ, 659, 122
Johnson, B., & Crotts, A. 2006, AJ, 132, 756
Kaiser, N. 2002, in Survey and Other Telescope Technologies and Discoveries, Proceedings of the SPIE, ed. J. A. Tyson, & S. Wolff, 4836, 154
Leibundgut, B. 2001, ARAA, 39, 67
Li, W., et al. 2001, PASP, 113, 1178
Li, W., et al. 2003, PASP, 115, 453
Lupton, R. H., Gunn, J. E., Ivezić, Ž., Knapp, G. R., Kent, S. M., & Yasuda, N. 2001, in ASP Conf. Ser. 238, Astronomical Data Analysis Software and Systems, ed. F. R. Harnden, F. A. Primini, & H. E. Payne (San Francisco, CA: ASP), 269
Miknaitis, G., et al. 2002, BAAS, 34, 1205
Miknaitis, G., et al. 2007, arXiv astro-ph/0701043
Oke, J. B., & Gunn, J. E. 1983, ApJ., 266, 713
Perlmutter, S., et al. 1999, ApJ, 517, 565
Pier, J. R., Munn, J. A., Hindsley, R. B., Hennessy, G. S., Kent, S. M., Lupton, R. H., & Ivezić, Ž. 2003, AJ, 125, 1559
Phillips, M. M., et al. 2007, PASP, 119, 360
Phillips, M. M., Lira, P., Suntzeff, N. B., Schommer, R. A., Hamuy, M., & Maza, J. 1999, AJ, 118, 1766
Poznanski, D., Gal-Yam, A., Sharon, K., Filippenko, A. V., Leonard, D. C., & Matheson, T. 2002, PASP, 114, 833
Prieto, J. L., et al. 2007, AJ, submitted (arXiv: 0704.0688)
Radburn-Smith, D. J., Lucey, J. R., & Hudson, M. J. 2004, MNRAS, 335, 1378
Riess, A. G., et al. 1998, AJ, 116, 1009
Riess, A. G., et al. 2004, ApJ, 607, 665
Riess, A. G., et al. 2007, ApJ, 659, 98
Sako, M., et al. 2005, in Proc. 22nd Texas Symposium on Relativistic Astrophysics, Stanford, CA, 2004 December, 13–17, arXiv astro-ph/0504455
Sako, M., et al. 2008, AJ, 135, 348
Schlegel, D. J., Finkbeiner, D. P., & Davis, M. 1998, ApJ, 500, 525
Smith, J. A., et al. 2002, AJ, 123, 2121
Sullivan, M., et al. 2006a, AJ, 131, 960
Sullivan, M., et al. 2006b, ApJ, 648, 868
Tyson, J. A. 2002, in Survey and Other Telescope Technologies and Discoveries, ed. J. A. Tyson, & S. Wolff, Proceedings of the SPIE, 4836, 10
Vanden Berk, D. E., Wilhite, B., Miceli, A., Stubbs, C., & Lawton, B. 2001, IAUC, 7744, 1
Wang, L., et al. 2005, BAAS, 37, 499
Wood-Vasey, W. M., et al. 2007, arXiv astro-ph/0701041
Woosley, S. E., & Bloom, J. S. 2006, ARAA, 44, 507
York, D. G., et al. 2000, AJ, 120, 1579
Zehavi, I., Riess, A. G., Kirshner, R. P., & Dekel, A. 1998, ApJ, 503, 483
Zheng, C., et al. 2007, AJ, submitted